*sustainability*

MDPI

*Article*

# Photoluminescent Applications for Urban Pavements

**Adriana H. Martínez *, Teresa López-Montero, Rodrigo Miró and Ricard Puig**

Road Research Laboratory, Universitat Politècnica de Catalunya-BarcelonaTech, 08034 Barcelona, Spain; teresa.lopez@upc.edu (T.L.-M.); r.miro@upc.edu (R.M.); ricard.puig.salesa@estudiantat.upc.edu (R.P.)
* Correspondence: adriana.martinez@upc.edu; Tel.: +34-93-401-72-73

**Abstract:** Photoluminescent materials used on street and road pavements could absorb solar energy during the day and emit it at night, which will save energy and improve visibility with a consequent improvement in road safety. The aim of this study is to evaluate the luminance of different photoluminescent applications for pavements (bituminous mixes, mortars, and paints) in which strontium aluminate and glass beads were used. Sunlight was simulated with two bulbs, one LED and one UV bulb, inside a measuring apparatus specially developed for this work. The luminance of the different designed solutions was determined at different time periods after their excitation. The results obtained showed that luminescent paints can reach higher luminance than bituminous mixes and mortars. The colour of the base surface on which the paints are applied had a great influence on the obtained luminance, which increases with the aluminate and glass beads content. Among all the solutions evaluated, the paint made with 60% aluminate and 6% glass beads, spread on a white surface, allowed the highest luminance values to be obtained. This study leads to the conclusion that it is possible to achieve a good photoluminescent level while economising on the amount of materials necessary.

**Keywords:** urban pavement; photoluminescence; bituminous mixture; mortar; paint

check for updates

**Citation:** Martínez, A.H.; López-Montero, T.; Miró, R.; Puig, R. Photoluminescent Applications for Urban Pavements. *Sustainability* **2023**, *15*, 15078. https://doi.org/10.3390/su152015078

Academic Editors: Laura Moretti and Paolo Peluso

Received: 16 September 2023
Revised: 10 October 2023
Accepted: 13 October 2023
Published: 20 October 2023

**Copyright:** © 2023 by the authors. Licensee MDPI, Basel, Switzerland. This article is an open access article distributed under the terms and conditions of the Creative Commons Attribution (CC BY) license (https://creativecommons.org/licenses/by/4.0/).

## 1. Introduction

It is evident that increasing the visibility of road signs can help to improve road safety. Some studies on lighting and road safety show that 90% of the information that a driver needs is acquired by sight and at night the eye suffers from a significant deficit of information [1–3]. There are a number of factors associated with traffic accidents at night, such as fatigue and increased speed, but visibility also plays an important role [4,5]. The driver's visual capacity is reduced to 20% with respect to daytime driving, and his or her ability to perceive distances and fields of vision is also reduced [6].

The severity of traffic accidents is usually higher during night-time driving than during daytime driving, as stated by Regev et al. [7]. In the specific case of Spain, the figures collected by Spain's Directorate General of Traffic indicate that the highest percentage of accidents does not occur during night-time driving, but it is when the highest percentage of fatal accidents occur. The accident fatality rate (the ratio between the number of deaths and accident victims) in Spain was 1.2 in 2019; however, in the case of night-time accidents (including dusk and dawn), this ratio reaches 1.69, which is 40% higher [8]. Studies from other countries have also shown that the accident and fatality rate in night-time driving can be as high as 1.6 times the daytime accident rate [9,10].

Guidelines for the design and implementation of horizontal road signage usually explain the daytime and night-time visibility characteristics of road markings. According to night-time visibility, these guides classify the markings into non-retroreflective and retroreflective markings [11]. Retroreflection is defined as the capacity that some surfaces have to reflect light in the direction of the emitting source, which allows road markings to be visible to drivers during the night when the vehicle's headlights are incident on the markings [12].

The materials used in these markings are considered as the "base", such as paints and thermoplastics, and the "post-mixing" materials include glass beads and non-slip aggregates [12]. The glass beads provide road markings with retroreflection, which is calculated as the ratio between the luminance of a marked area of road in one given direction and the illuminance of that area [13].

For its part, luminance can be defined as the brightness intensity of a material and is the result of dividing the luminous intensity of a surface by its area of incidence in a given direction [14]. The signage guide explains that the luminances from a vehicle's headlights are generally small and states a normal range between 0.001 cd/m$^2$ and 0.100 cd/m$^2$. To increase the retroreflection of road markings, glass beads are usually used that intensify the visual stimulus so that relatively small objects can be seen [15].

An alternative base material to those commonly used, which would provide a greater degree of visibility for road users, including both drivers and pedestrians, is a material that is photoluminescent. Photoluminescent materials emit light as a result of the release of energy due to the absorption of photons [16–20]. During stimulation (exposure to the sun), the absorbed energy stimulates electronic transitions to higher energy states (excited state). When the stimulation ends, the electron falls from the excited state to a lower energy state, releasing the energy in the form of light. Depending on the lifetime of the emitted luminescence, photoluminescent materials can be classified as fluorescent (average life < 10 ms) or phosphorescent (average life $\geq$ 0.1 s) [21]. The design of materials with photoluminescent properties for use in pavements has focused on phosphorescent-type materials; that is, those that emit light once the excitation has ceased.

In the 1990s, materials called "long-lasting phosphors" were discovered and products with high emission power and long decay times were obtained, such as strontium aluminate, which is a yellow, odourless, and non-flammable monoclinic crystalline powder [22]. This heavier-than-water compound is chemically and biologically inert. When activated with the appropriate dopant, it behaves as a photoluminescent phosphor. Currently, the most commonly found phosphorescent materials are strontium aluminates europium and dysprosium doped ($SrAl_2O_4$:$Eu^{2+}$,$Dy^{3+}$), which emits in green, and calcium aluminates europium and neodymium doped ($CaAl_2O_4$:$Eu^{2+}$,$Nd^{3+}$), which emits in blue. Currently, these are used in exit signs, road signage, and other safety-related signs. Thus, photoluminescent signage must comply with standard UNE 23035-1.

The use of materials with photoluminescent properties on the surface course of road pavements or bicycle lanes is a very attractive idea as they are capable of absorbing solar energy during the day in order to emit it during the night.

Luminance is a key factor in these types of materials, which depends on the type of surface and illumination source, and the unit of measurement is the candela per square metre (cd/m$^2$). For its part, illuminance refers to the light intensity that is incident on a surface, measured in lux. According to Andre and Owens [23], the minimum night-time visibility in many road safety applications is 3.3 lx, while the illuminance in many indoor illumination applications is normally around 300 lx.

As Bachanek et al. reported, global consumption of electricity is reaching considerable sums and increases by around 3% every year [24]. Outdoor illumination is responsible for 15–19% of this consumption and illumination represents 2.4% of humanity's annual energy resources, and is responsible for 5–6% of the total greenhouse gas emissions to the atmosphere [25,26].

Sadeghian et al. reviewed the energy-saving options in the electrical distribution grid for buildings and public lighting systems [27]. They analysed the energy and emissions savings potential of a series of prior studies with different alternatives, concluding that there are potential solutions for reducing energy consumption.

Recently, Belloni et al. developed an intelligent illumination system based on blue diode laser technology combined with photoluminescent pavements to obtain a self-illuminating surface [28]. Even though this application is still a prototype, the results indicate promising benefits in terms of electricity saving and uniformity of luminance.

Many cities and municipalities throughout the world are starting to explore intelligent city options for the illumination of public spaces. Notable among the most innovative are those that study the possibility of replacing or supporting artificial street lighting by means of bioluminescence, with transgenic bioluminescent plants [29] and marine bacteria [30].

Studies relating to photoluminescence on road pavements have focused on a photoluminescent coating on the top layer of the bituminous mix. Praticò et al. studied the photoluminescence phenomenon in terms of loading and unloading according to the type of pavement (dense or gap-graded bituminous mixes), and the paint treatment by applying a coating with photoluminescent properties on the top layer of the pavement [31]. Gutiérrez and Colorado developed a photoluminescent coating made from strontium aluminate and expanded polyethylene waste for use in asphalt pavements and obtained acceptable mechanical properties [32].

Giulinai and Auteliano analysed the use of photoluminescent pigments for thin surface courses based on zinc sulphide (ZnS:Cu) and on strontium aluminate ($SrAl_2O_4$:$Eu^{2+}$,$Dy^{3+}$) under different experimental conditions [33]. They concluded that the selection of photoluminescent pigments should favour materials capable of absorbing radiation from sunlight and re-radiating it at wavelengths visible to the human eye for appreciable periods of time.

Chiatti et al. published a study in which they researched innovative solutions for achieving luminescent and reflective results at the same time [34]. They used paints with different coloured pigments from the strontium aluminate, calcium aluminate and silicate family, all doped with europium, in order to obtain different colours. They statistically verified that the attenuation of the luminance varied with the chemical composition of each pigment. The results indicated that the europium-doped strontium aluminate reached much higher radiance and luminance values than the other two compounds.

The application of photoluminescent elements on Portland cement for pavement concretes has also been studied, as in the works of Sanjuán and Argiz or Rosas-Casares et al., for example [35,36].

Similarly, the aim of this study is to analyse the effectiveness of different applications for pavement surfaces from the luminance point of view, including bituminous mixes as well as bituminous mortars and paints, and to compare the results obtained.

## 2. Materials and Methods

### *2.1. Materials*

Three different applications have been studied: bituminous mixes, bituminous mortars, and paints, to which photoluminescent materials have been added. Even though the initial hypothesis assumed that the luminescent effect would only be seen on a small thickness of the surface, whether it makes sense to consider a greater thickness that provides higher luminescence has been analysed. This is the reason why three different applications of significantly different thicknesses were designed.

#### 2.1.1. Bituminous Mixes

Two bituminous mixes were manufactured with white limestone aggregate, which were basically differentiated by the gradation used (see Figure 1). Mix 1 was dosed with a higher quantity of fine aggregate than mix 2 (see Table 1). The bitumen used in both mixes was a light-coloured synthetic binder (semi-transparent) at 6.5% by weight of the aggregate. Table 2 shows the characteristics of the synthetic bitumen, together with those of the conventional bitumen used in mortars.

As can be seen in Figure 1, the texture obtained on both specimens is very different, due to the difference in the gradation of the aggregates.

(**a**) (**b**)

**Figure 1.** Specimens manufactured with white limestone aggregate, strontium aluminate and glass beads. (**a**) mix 1 and (**b**) mix 2.

**Table 1.** Dosages of the bituminous mixes.

| Mixture | 1 | 2 |
|---|---|---|
| Coarse aggregate (%) | 28.5 | 47.5 |
| Fine aggregate (%) | 38.6 | 20 |
| Strontium aluminate (%) | 26.5 | 26.5 |
| Glass beads 250 µm (%) | 6.4 | 6.4 |

**Table 2.** Characteristics of the bitumens used in mixtures and mortars.

| Characteristic | Synthetic * | 50/70 |
|---|---|---|
| Density (g/cm$^3$) | 0.95–1.15 | |
| Penetration at 20 °C (0.1 mm) | 20–50 | 61 |
| Softening Point R&B (°C) | ≥85 | 50.9 |
| Fraass breaking point (°C) | ≤−20 | −14 |
| Flash Point (°C) | ≥270 | 280 |
| **Residue after Ageing** | | |
| Mass variation (%) | ≤1.5 | 0.1 |
| Penetration at 25 °C (% o.p.) | ≥80 | 66 |
| Softening Point increase (°C) | ≤10 | 7.6 |

*: provided by the supplier.

### 2.1.2. Bituminous Mortars

Four bituminous mortars were manufactured, dosed with white limestone and dark grey porphyry aggregates, with a maximum size of 4 mm and a variation of the dosages of strontium aluminate and glass beads (see Table 3). The mortars are identified as A and B. A1 and B1 are mortars with limestone aggregate, and A2 and B2 are mortars with porphyry aggregate (see Figure 2). In all the mortars, the synthetic bitumen content was 20% of the aggregate weight.

**Table 3.** Dosages of the bituminous mortars.

| Mortar | A | | B | |
|---|---|---|---|---|
| | A1 | A2 | B1 | B2 |
| Aggregate type | limestone | porphyry | limestone | porphyry |
| Aggregate (%) | 35 | | 60 | |
| Strontium aluminate (%) | 50 | | 30 | |
| Glass beads (%) | 15 | | 10 | |

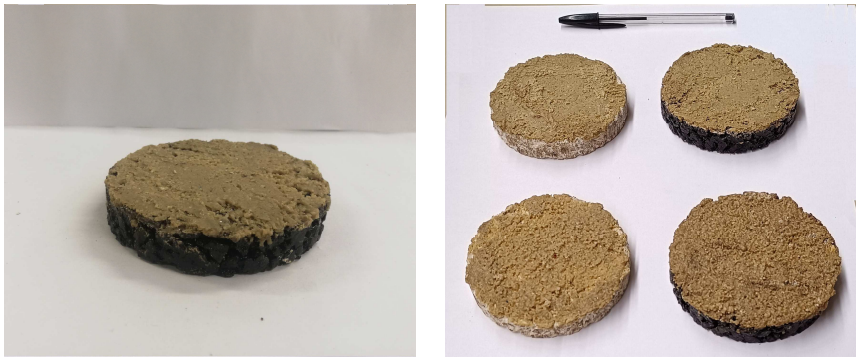

(**a**) (**b**)

**Figure 2.** Bituminous mortars: (**a**) appearance of the mortar on the base specimen, (**b**) combinations of mortars on the base specimens.

Mortars A1 and B1 were spread over the specimens prepared with limestone aggregate and synthetic bitumen, while mortars A2 and B2 were spread over specimens prepared with porphyry aggregate and conventional bitumen.

#### 2.1.3. Luminescent Paints

With respect to the luminescent paints, they were manufactured from a mix of resin, strontium aluminate and glass beads, which were combined in different dosages and applied on different bituminous surfaces. The dosages used for the paints are included in Table 4.

**Table 4.** Dosages of the studied paints (by weight).

| No | Series | Resin (%) | Aluminate (%) | Glass Beads (%) |
|---|---|---|---|---|
| 1 | 20-0 | 80 | 20 | 0 |
| 2 | 20-6 | 74 | 20 | 6 |
| 3 | 20-12 | 68 | 20 | 12 |
| 4 | 40-0 | 60 | 40 | 0 |
| 5 | 40-6 | 54 | 40 | 6 |
| 6 | 40-12 | 48 | 40 | 12 |
| 7 | 60-0 | 40 | 60 | 0 |
| 8 | 60-6 | 34 | 60 | 6 |
| 9 | 60-12 | 28 | 60 | 12 |

The resin used is a styrene acrylic copolymer based on a transparent thermoplastic solvent. The glass beads have a diameter of 250 microns.

The different bituminous surfaces were obtained from specimens of different mixes on which the paints were applied. These base specimens were manufactured with two types of aggregate, limestone and porphyry, and two types of bitumen, synthetic and 50/70, respectively, in order to be able to assess the effect of the colour of the underlying layer. When the limestone aggregate and synthetic bitumen mix were used, 2% titanium dioxide was added to obtain a colour closer to white. A third surface was also prepared based on a bituminous mix manufactured with porphyry aggregate and 50/70 bitumen, the surface of which was painted white (with conventional paint), which allowed an intermediate colour to be obtained between the aforementioned white and black (see Figure 3).

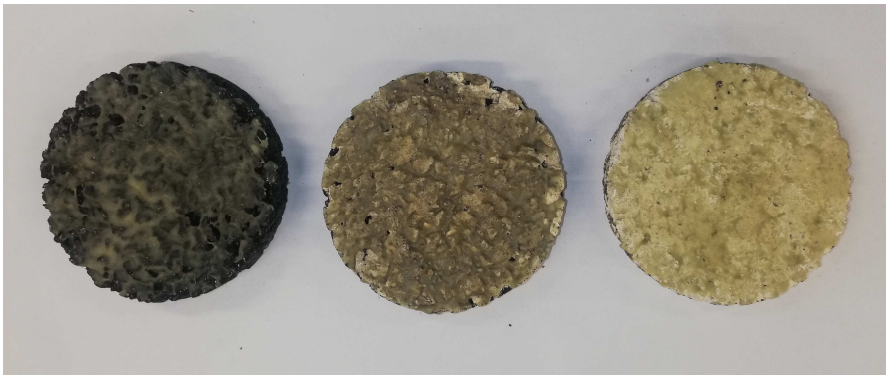

(**a**) (**b**) (**c**)

**Figure 3.** Paints applied on specimens prepared with: (**a**) porphyry aggregate (black), (**b**) porphyry aggregate with white paint (grey), (**c**) limestone aggregate (white).

In this way, 3 different coloured surfaces were obtained, which from now on are called white, grey and black, on which 9 paints were applied with different dosages, thus obtaining a total of 27 series. The letter that identifies the type of surface has been added to the denomination indicated in Table 4. W (white), G (grey) and B (black).

### *2.2. Methods*

As regards the measurement of luminous properties, in general the procedure described in standard UNE-23035-1 [37] for products used in luminescent signs has been followed. The luminance was measured during the attenuation time as well as the attenuation time itself, although some modifications have been introduced.

As has been mentioned, luminance is the luminous intensity radiated per apparent surface unit of a body that emits light and is usually expressed in millicandelas per square metre, mcd/m$^2$. The attenuation time is that elapsed from the end of the stimulation until the luminance is reduced to 0.3 mcd/m$^2$.

The luminance, according to this standard, is measured by stimulating the surface to be measured with a Xenon light that emits an illuminance of 1000 lux for 5 min, after which the luminance measurement process is begun. The luminance is measured as a function of time (up to 120 min) and an attenuation time is determined until a value of 0.3 mcd/m$^2$ is measured. The procedure to be followed consists of representing the luminance values on a logarithmic scale and extrapolating linearly until 0.3 mcd/m$^2$ is reached, at which point the corresponding time is recorded.

Given the current difficulty of finding Xenon lights, the studies carried out by Giuliani and Autelitano were considered [33], where a combination of an LED lamp and a UV lamp was used, both 5 W, and the surface and the bulbs were placed inside a tube so that the luminous capacity was not dispersed.

To establish the stimulation time, the work carried out by Gao et al. was considered in which it was observed that a time greater than 30 min no longer had an effect on luminance [38]. To confirm this stimulation time value, the luminances obtained on the mix 1 specimen exposed to sunlight were compared with the same specimen exposed to UV and LED lamps at different times (5 and 30 min), and it was concluded that an equivalent effect was obtained after 30 min (see Figure 4).

The distance was also calculated at which the lamps had to be located in order to achieve 1000 lux. For this, the illuminance was measured at a certain distance and the inverse square law of the distance was used, which defines the relationship between the illuminance and the measurement surface with respect to the light source, and the result was a distance of 31.5 cm. Table 5 includes the illuminances when the tube is used and not used, highlighting the fact that the tube prevents the dispersion of the illumination, as previously mentioned.

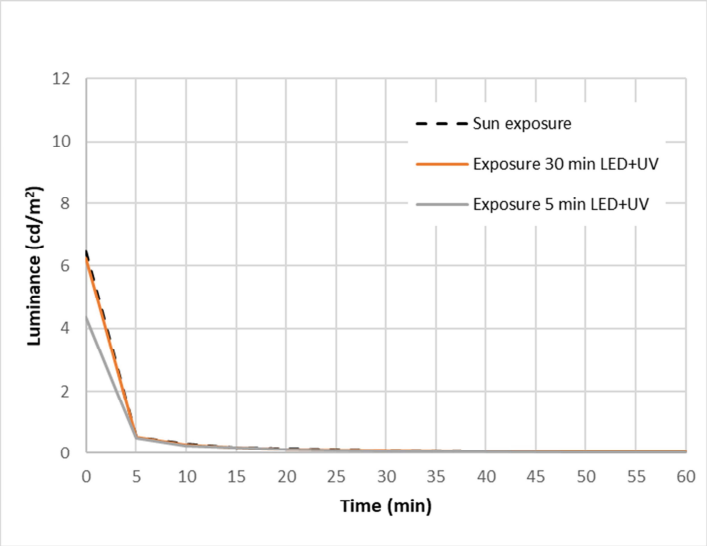


**Figure 4.** Evolution of the luminance with attenuation time of the specimen exposed to solar radiation and different stimulation times of the lamp combination.

**Table 5.** Measured illuminances recorded at different distances from the emitting source.

| Height (cm) | Illuminance Outside the Tube (lux) | Illuminance Inside the Tube (lux) |
|---|---|---|
| 30 | 670 | 1100 |
| 35 | 476 | 788.5 |
| 40 | 275 | 631 |

To carry out the luminance measurements, a Konica Minolta brand LS-150 luminance meter was used with a close-up lens that was placed at a distance of 53 cm from the surface to be measured.

Five reading points arranged in a cross were considered on each surface to be measured, which allowed the average value at the different measurement times to be obtained: 0, 5, 10, 15, 20, 30, 40, 50, and 60 min.

## 3. Results

### *3.1. Bituminous Mixtures*

The attenuation curves of the studied mixes are presented in Figure 5. These curves describe the decay of the luminance over time. A rapid drop can be seen in the first stage which takes place over the first few minutes, followed by a slow drop which extends over a longer period of time.

For the mix 1 specimen, the luminance value recorded at the initial moment was 4.36 cd/m$^2$, while for the mix 2 specimen it was 2.1 cd/m$^2$. The aggregate gradation of mix 1 allowed a more closed specimen to be manufactured with less texture and, therefore, a larger area to emit light. These results agree with the research carried out by Practicò et al. on dense and open asphalt specimens [31].

Although it was not possible to measure macrotexture according to EN 13036-1 [39] because the surface area required to perform this test is larger than that of the flat side of the specimens, it was estimated following the method proposed by Practicò and Astolfi for Marshall specimens [40]. The macrotexture of specimen 1 was less than 0.5 mm (the exact value could not be determined due to limitations of the specimen dimensions) and specimen 2 had a macrotexture of 0.9 mm.

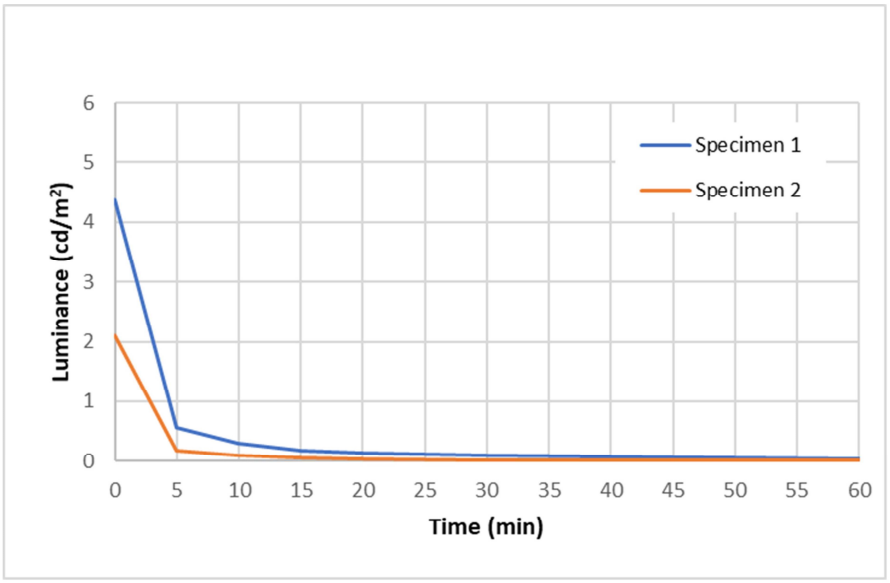


**Figure 5.** Luminance values recorded for the bituminous mix specimens.

### *3.2. Bituminous Mortars*

The results plotted on the graph in Figure 6 (note the detail in the inset plot) show that all the mortars spread on limestone aggregate have higher luminance at the initial instant than when spread on porphyry aggregate and, for all the bases, the mortar with the highest aluminate and bead content has the highest luminance. The maximum luminance value at the initial instant is 3.26 cd/m$^2$ for the A1 mortar, with the highest aluminate and bead content, spread over limestone aggregate, while the minimum value is 1.88 cd/m$^2$ for the B2 mortar, manufactured with the lowest aluminate and bead content, spread over porphyry aggregate.

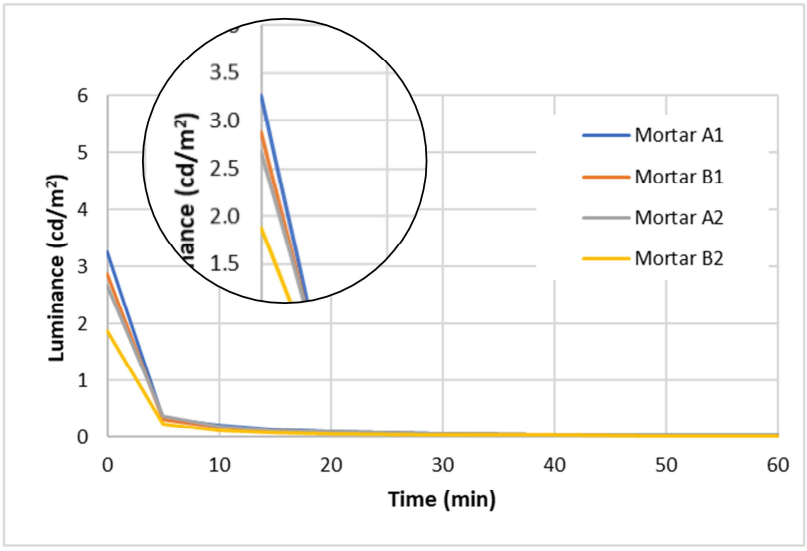


**Figure 6.** Luminous values recorded for the bituminous mortars.

The difference in luminance between the results of specimens and mortars is explained by the fact that a higher binder content was used in the mortars, which darkened the surface colour, resulting in a lower luminance. Based on these results, and with the intention of further reducing the thickness of the luminescent application, it was decided to study paints made with transparent resin instead of synthetic bitumen, in order to achieve lighter surfaces.

### *3.3. Luminescent Paints*

The next stage focused on the study of different paint dosages applied on different bituminous surfaces. Given that nine series were analysed on three different surfaces (white, grey and black), the overall results obtained are presented below and are analysed consecutively for each type of surface.

Figure 7 shows the results obtained for the paint with the intermediate dosage of aluminate (40%) and beads (6%) on the three surfaces. The effect of the surface colour has a significant influence on the luminance over the whole measurement time (see Figure 8).

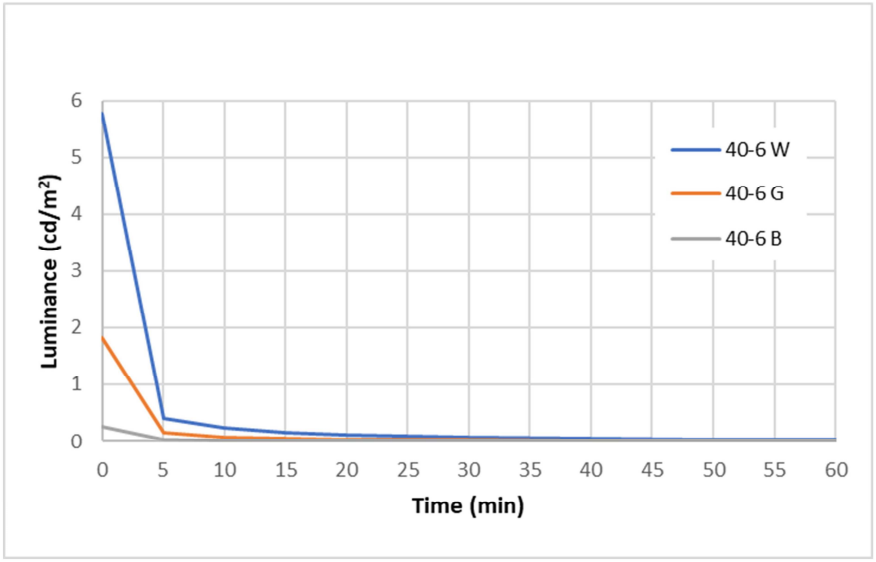


**Figure 7.** Luminance values recorded for the paint with 40% aluminate and 6% glass beads on the three studied surfaces.

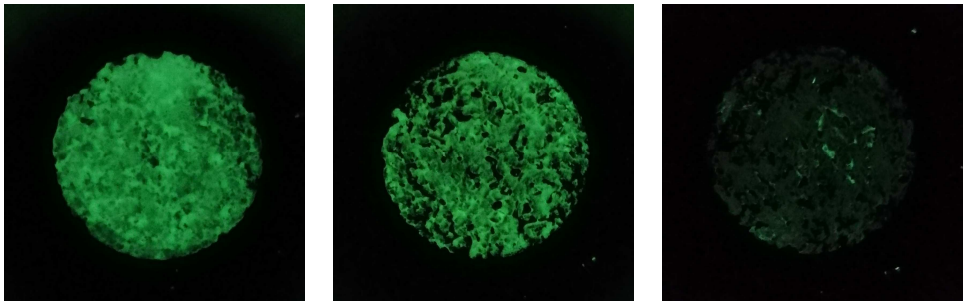

(**a**) (**b**) (**c**)

**Figure 8.** Images of surfaces after stimulation: (**a**) 40-6 W, (**b**) 40-6 G, (**c**) 40-6 B.

Figure 9 includes the luminance values on all the paint and surface combinations, measured at 0, 5 and 20 min. The effect of the different aluminate and bead dosages is evident, but so is the type of surface on which the paints are applied. The luminance values of all the paints on the white surface are always higher than the paints on the grey surface, and these in turn are higher than those on the black surface. For each surface, the luminance values increase with the aluminate content and, in general, with the glass bead content, up to a point at which the luminance starts to decay with higher bead content. This shows that there must be an optimal bead content, the arrangement of which allows the luminance to be maximised.

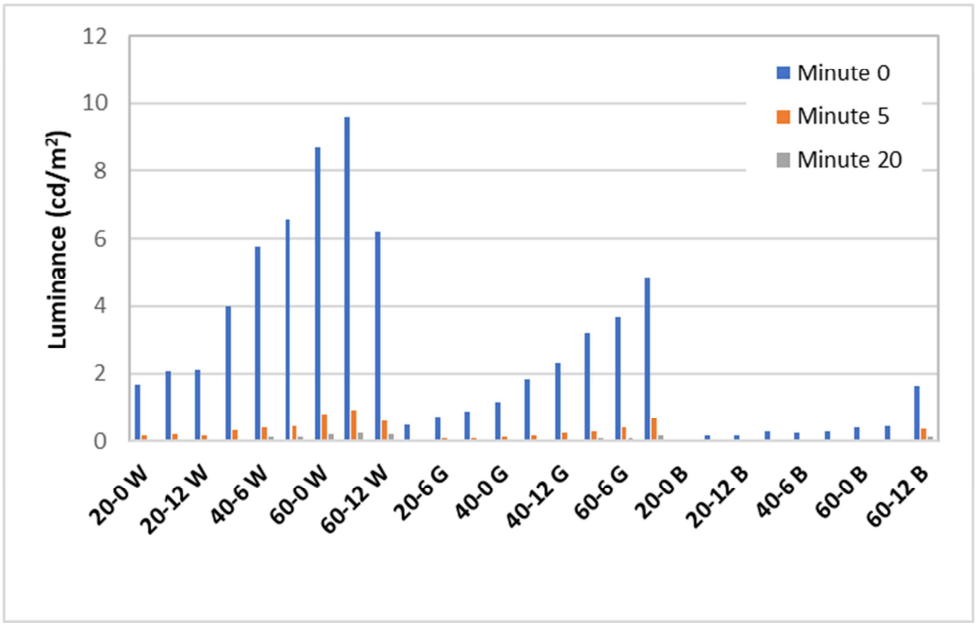


**Figure 9.** Luminance at instants 0, 5, and 20 min for all the analysed paints.

In the first instant, the luminance values vary between a minimum of 0.063 cd/m$^2$ for the case of the paint with the least aluminate content and with no beads on a black surface (20-0 B) and a maximum of 9.6 cd/m$^2$ for the case of the paint with 60% aluminate and 6% beads on the white surface (60-6 W).

The luminance values of all the paints applied on each one of the surfaces have been represented in Figures 10–12.

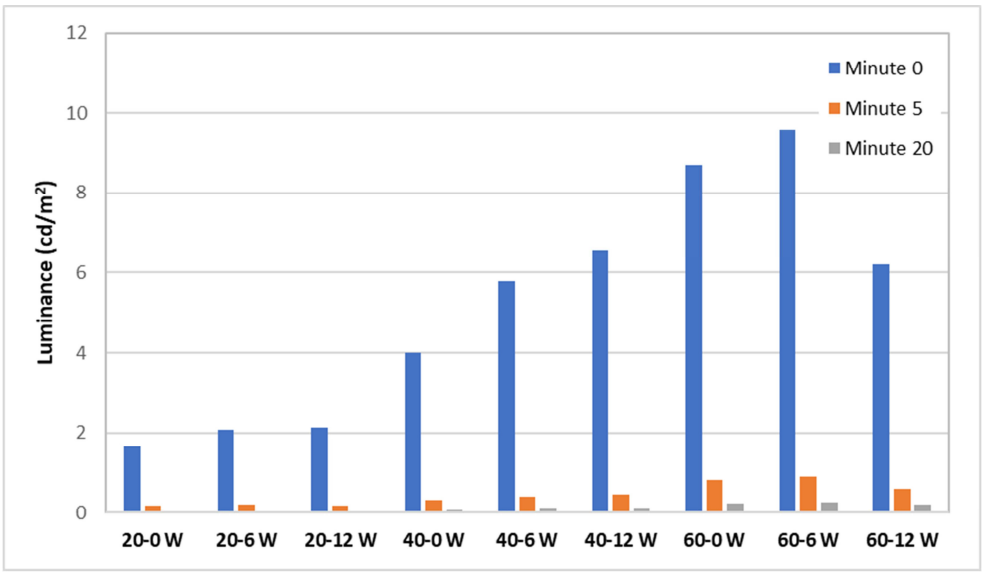


**Figure 10.** Luminance at instants 0, 5, and 20 min for all the paints applied on white surfaces.

As has been mentioned, the paints applied on white surfaces showed the highest initial luminance values, which generally increased with the aluminate and glass bead content (see Figure 10), except in the case of the maximum bead content with the maximum aluminate content, where the luminance values start to decrease (60-12 W).

The influence of strontium aluminate and glass beads content was determined by a two-way Analysis of Variance (ANOVA). The *p*-values obtained (significance level of 95%) in Table 6 indicate that both factors, as well as the interaction between them, have a signifi-

cant effect on luminance values (the significance was defined based on a $p$-value < 0.05, i.e., 95% confidence level).

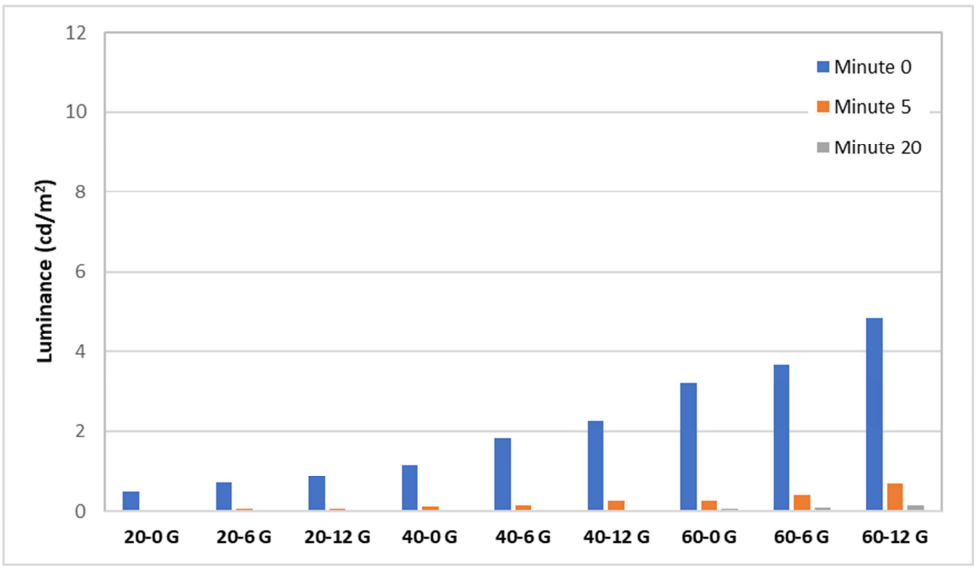


**Figure 11.** Luminance at instants 0, 5 and 20 min on grey surfaces (black surfaces painted white).

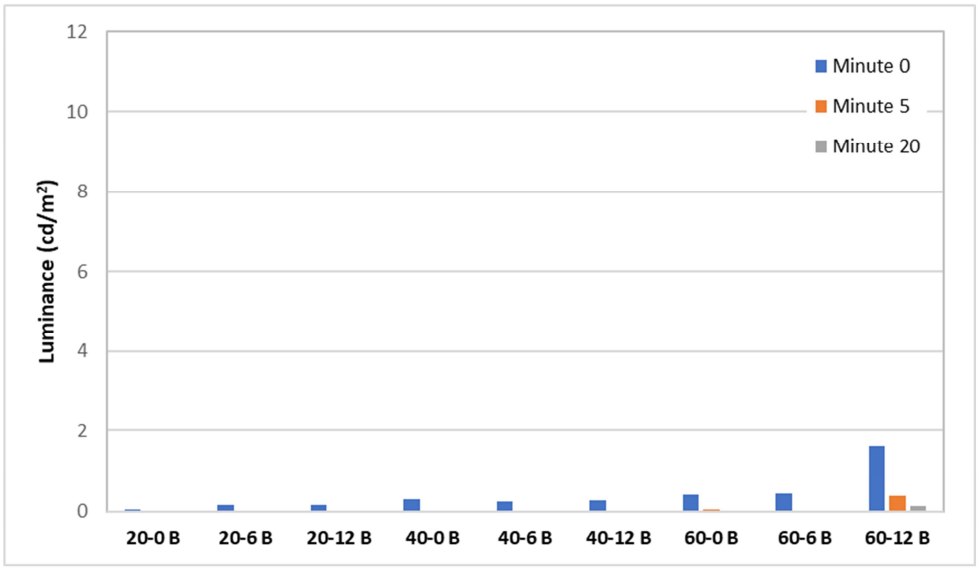


**Figure 12.** Luminance at instants 0, 5, and 20 min for all the paints applied on black surfaces.

**Table 6.** Two-way ANOVA for paints applied on white surfaces.

| Source | DF | Adj SS | Adj MS | F-Value | *p*-Value |
|---|---|---|---|---|---|
| Aluminate | 2 | 263.06 | 131.532 | 144.85 | 0.000 |
| Glass beads | 2 | 16.67 | 8.335 | 9.18 | 0.001 |
| Aluminate * Glass beads | 4 | 45.54 | 11.385 | 12.54 | 0.000 |
| Error | 36 | 32.69 | 0.908 | | |
| Total | 44 | 357.96 | | | |

*: interaction between Aluminate and Glass beads.

In the case of the paints on the grey surface, the luminance values varied between 29 and 78% of the values recorded in the case of the white surfaces (see Figure 11). In this case, a drop in the luminance is not observed when using 60% aluminate and 12% glass

beads (60-12 G), probably because the maximum bead content for this series is higher due to the colour difference of the surface.

Again, ANOVA found significant differences in the content of both components and also in the interaction between them, as can be seen in Table 7.

**Table 7.** Two-way ANOVA for paints applied on grey surfaces.

| Source | DF | Adj SS | Adj MS | F-Value | *p*-Value |
|---|---|---|---|---|---|
| Aluminate | 2 | 80.115 | 40.0577 | 212.34 | 0.000 |
| Glass beads | 2 | 8.361 | 4.1804 | 22.16 | 0.000 |
| Aluminate * Glass beads | 4 | 2.415 | 0.6038 | 3.2 | 0.024 |
| Error | 36 | 6.791 | 0.1886 | | |
| Total | 44 | 97.683 | | | |

*: interaction between Aluminate and Glass beads.

Finally, the paints applied on the black surfaces are those that show the lowest luminance values, between 4 and 25% of the values obtained when using the specimens with a white surface (see Figure 12). The last series (60-12 B) has luminance values higher than the rest, because the amount of paint applied was higher than for the rest of the series and, therefore, this value should not be taken into account for the overall analysis.

Table 8 shows the ANOVA test for these last types of paints, indicating similar trends to those seen with white and grey base surfaces.

Additionally, all the luminance values recorded were used for determining the attenuation time by extrapolation. In accordance with standard UNE-23035-1, the most restrictive minimum luminance values are those required for photoluminescent pigments for use in signs, which are:

Luminance at 10 min $\geq$ 60 mcd/m$^2$
Luminance at 60 min $\geq$ 7.8 mcd/m$^2$
Attenuation time (0.3 mcd/m$^2$) $\geq$ 900 min.

Figure 13 shows the extrapolation of the luminance for the 60-6 W series. It can be observed that the analysed series meets the requirements of the standard because after 10 and 60 min, the luminance exceeds the minimum values required and 0.3 mcd/m$^2$ is reached after 900 min.

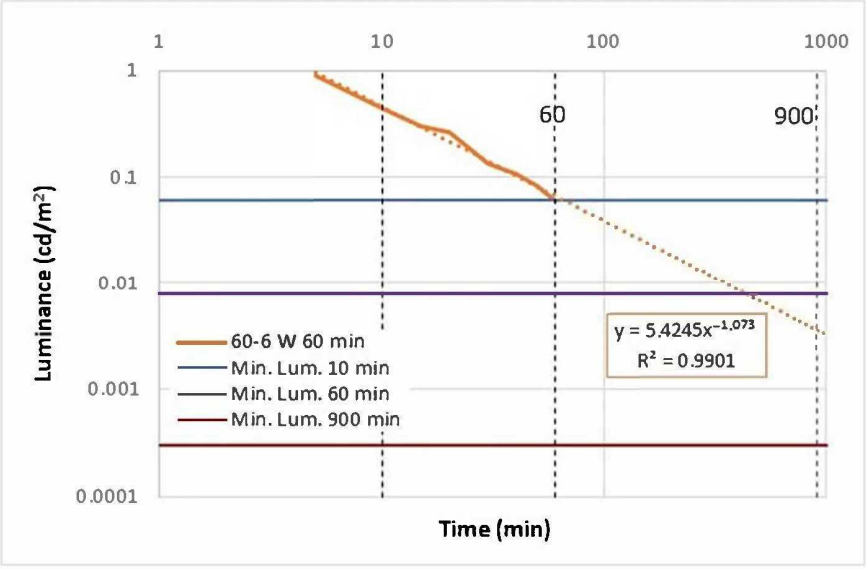


**Figure 13.** Extrapolation of the luminance for the 60-6 W series.

**Table 8.** Two-way ANOVA for paints applied on black surfaces.

| Source | DF | Adj SS | Adj MS | F-Value | *p*-Value |
|---|---|---|---|---|---|
| Aluminate | 2 | 4.154 | 2.07713 | 52.53 | 0.000 |
| Glass beads | 2 | 1.68 | 0.83977 | 21.24 | 0.000 |
| Aluminate * Glass beads | 4 | 3.005 | 0.75128 | 19 | 0.000 |
| Error | 36 | 1.424 | 0.03954 | | |
| Total | 44 | 10.263 | | | |

*: interaction between Aluminate and Glass beads.

This task was carried out for all the studied series and the results are included in Table 9, with an indication of whether each criterion is met or not.

**Table 9.** Analysis of the studied photoluminescent paint according to the criteria established in standard UNE-23035-1 for photoluminescent pigments.

| Series | Criterion | White Base | Grey Base | Black Base |
|---|---|---|---|---|
| 20-0 | Min Lum. 10 min | ✓ | x | x |
| | Min Lum. 60 min | ✓ | x | x |
| | Decay time | ✓ | x | x |
| 20-6 | Min Lum. 10 min | ✓ | x | x |
| | Min Lum. 60 min | ✓ | x | x |
| | Decay time | ✓ | x | x |
| 20-12 | Min Lum. 10 min | ✓ | x | x |
| | Min Lum. 60 min | ✓ | x | x |
| | Decay time | ✓ | ✓ | x |
| 40-0 | Min Lum. 10 min | ✓ | ✓ | x |
| | Min Lum. 60 min | ✓ | ✓ | x |
| | Decay time | ✓ | ✓ | x |
| 40-6 | Min Lum. 10 min | ✓ | ✓ | x |
| | Min Lum. 60 min | ✓ | ✓ | x |
| | Decay time | ✓ | ✓ | x |
| 40-12 | Min Lum. 10 min | ✓ | ✓ | x |
| | Min Lum. 60 min | ✓ | ✓ | x |
| | Decay time | ✓ | ✓ | ✓ |
| 60-0 | Min Lum. 10 min | ✓ | ✓ | x |
| | Min Lum. 60 min | ✓ | ✓ | x |
| | Decay time | ✓ | ✓ | ✓ |
| 60-6 | Min Lum. 10 min | ✓ | ✓ | x |
| | Min Lum. 60 min | ✓ | ✓ | x |
| | Decay time | ✓ | ✓ | ✓ |
| 60-12 | Min Lum. 10 min | ✓ | ✓ | ✓ |
| | Min Lum. 60 min | ✓ | ✓ | ✓ |
| | Decay time | ✓ | ✓ | ✓ |

The results show that the paints applied on white surfaces meet the three criteria established by standard UNE-23035-1, 60-6 W being the paint which allows the highest values of luminance to be obtained. In the case of grey surfaces (black surfaces painted white), the criteria are not met when the lowest content of aluminate is used (20%), and when the base surface is black, practically none of the paints comply, with the exception of the series that contains the highest aluminate and bead content (60% and 12%, respectively). It is evident that both the quantity of aluminate and beads as well as the colour of the base surface influence the results obtained, even though it is possible to neutralise the effect of the dark surfaces (grey and black) with a larger quantity of aluminate and beads.

## 4. Conclusions

This study analyses the feasibility of using photoluminescent materials to partially or totally replace artificial illumination as a sustainable alternative to reduce the consumption of electrical energy and decarbonise outdoor urban environments, at the same time as improving road safety.

The results obtained allow the following conclusions to be made:

- For the bituminous mixes, texture is a key factor in the luminance value obtained. It was observed that most closed surfaces can achieve double the initial luminance value for the same content of aluminate and glass beads.
- The bituminous mortars show that the higher the aluminate and glass beads content, the higher the luminance, although the colour of the base also has an influence with clear bases having higher luminance.
- It was observed that the effect of the base surface colour is more significant for the paints than for the mortars, and higher luminance values were obtained for the light bases. For the same base, in general, the luminances increase with the aluminate and glass bead content, except for very high bead values combined with very high aluminate values, in which case the luminance value starts to decay. Paint 60-6 W has the dosage that allows the highest luminance values to be obtained.

Finally, it has been shown that the luminescent paints applied on light surfaces can reach luminance values higher than those obtained by means of bituminous mixes and mortars, making it possible to achieve a good photoluminescent level while economising on the amount of materials necessary.

Photoluminescent mixes can be considered the new materials of the future due to their numerous benefits for society. Not only do they improve night-time visibility, but they also save energy because public lighting in city streets can be reduced, thus contributing to the mitigation of the urban heat island effect, considered a key issue for sustainable development.

**Author Contributions:** Conceptualization, R.M., T.L.-M. and A.H.M.; methodology, R.M.; formal analysis, A.H.M. and T.L.-M.; investigation, R.M., A.H.M., T.L.-M. and R.P.; resources, A.H.M. and R.M.; data curation, T.L.-M., R.P. and A.H.M.; writing—original draft preparation, A.H.M.; writing—review and editing, R.M. and T.L.-M.; visualization, R.M., T.L.-M. and R.P.; funding acquisition, T.L.-M., R.M. and A.H.M. All authors have read and agreed to the published version of the manuscript.

**Funding:** This publication is part of the R&D&I project "Heat island mitigation to prevent global warming by designing sustainable pavements with reflective and photoluminescent properties (RELUM)", supported by grant TED2021-132077B-I00, funded by MCIN/AEI/10.13039/501100011033/ and by the European Union "NextGenerationEU/PRTR".

**Institutional Review Board Statement:** Not applicable.

**Informed Consent Statement:** Not applicable.

**Data Availability Statement:** The data presented in this study are available on request from the corresponding author.

**Acknowledgments:** Teresa López-Montero is a Serra Húnter Fellow.

**Conflicts of Interest:** The authors declare no conflict of interest.

## References

1. North, R.V. *Work and the Eye*; Oxford University Press: Oxford, UK, 1993; ISBN 0192618857.
2. Florida Department of Transportation. Defensive Driving Computer-Based Training. Module 5. Visual Search. Available online: http://wbt.dot.state.fl.us/ois/DefensiveDriving/pdf/Module05.pdf (accessed on 30 September 2023).
3. Chen, H.; Fanny, K. Understanding the contributing factors to nighttime crashes at freeway mainline segments. *J. Transp. Technol.* **2019**, *9*, 450–461. [CrossRef]
4. Åkerstedt, T.; Kecklund, G.; Hörte, L.G. Night driving, season, and the risk of highway accidents. *Sleep* **2001**, *24*, 401–406. [CrossRef] [PubMed]

5. Konstantopoulos, P.; Chapman, P.; Crundall, D. Driver's visual attention as a function of driving experience and visibility. Using a driving simulator to explore drivers' eye movements in day, night and rain driving. *Accid. Anal. Prev.* **2010**, *42*, 827–834. [CrossRef] [PubMed]
6. Estudio RACE: Iluminación del Automóvil y Seguridad Vial, 2006. Real Automóvil Club de España (RACE). Available online: https://revista.dgt.es/es/reportajes/2021/12DICIEMBRE/1214-Conduccion-nocturna.shtml (accessed on 9 August 2023).
7. Regev, S.; Rolison, J.J.; Moutari, S. Crash risk by driver age, gender, and time of day using a new exposure methodology. *J. Saf. Res.* **2018**, *66*, 131–140. [CrossRef]
8. DiConsejos para Conducir de Noche, Nota del 12/01/2022. Dirección General de Tráfico. Available online: https://www.dgt.es/comunicacion/noticias/consejos-para-conducir-de-noche/ (accessed on 10 August 2023).
9. National Highway Traffic Safety Association (NHTSA). *Passenger Vehicle Occupant Fatalities by Day and Night—A Contrast*; National Highway Traffic Safety Administration: Washington, DC, USA, 2007.
10. Hawkins, N.; Hallmark, S.; Smadi, O.; Kinsenbaw, C.; Orellana, M.; Hans, Z.; Isebrands, H. *Strategies to Address Nighttime Crashes at Rural, Unsignalized Intersections. Final Report*; Center for Transportation Research and Education, Iowa State University: Ames, IA, USA, 2008.
11. Dirección General de Carreteras. *Guía para el Proyecto y Ejecución de Obras de Señalización Horizontal*; Ministerio de Fomento: Madrid, Spain, 2012; ISBN 978-84-498-0926-2.
12. Bahar, G.; Masliah, M.; Erwin, T.; Tan, E.; Hauer, E. *Pavement Marking Materials and Markers: Real-World Relationship between Retroreflectivity and Safety over Time*; The National Academies Press: Washington, DC, USA, 2006; No. Project 17-28.
13. Thamizharasan, A.; Sarasua, W.A.; Clarke, D.B.; Davis, W.J. A Methodology for Estimating the Lifecycle of Interstate Highway Pavement Marking Retroreflectivity. In Proceedings of the 83rd Transportation Research Board Annual Meeting, Washington, DC, USA, 11–15 January 2004; TRB Paper Number: 03-3867.
14. Austin, R.L.; Schultz, R.J. *Guide to Retroreflection Safety Principles and Retrorereflective. Measurements*; Gamma Scientific: San Diego, CA, USA, 2020; ISBN 0-9710215-0-3.
15. European Cooperation in the Field of Scientific, & Technical Research (Organization). *COST 331: Requirements for Horizontal Road Marking: Final Report of the Action*; Office for Official Publications of the European Communities: Luxembourg, 1999; Volume 331.
16. Rojas-Hernández, R.E.; Rubio-Marcos, F.; Rodríguez, M.Á.; Fernández, J.F. Long lasting phosphors: $SrAl_2O_4$: Eu, Dy as the most studied material. *Renew. Sustain. Energy Rev.* **2018**, *81*, 2759–2770. [CrossRef]
17. Kaya, S.Y.; Karacaoglu, E.; Karasu, B. Effect of Al/Sr ratio on the luminescence properties of $SrAl_2O_4$: $Eu^{2+}$, $Dy^{3+}$ phosphors. *Ceram. Int.* **2012**, *38*, 3701–3706. [CrossRef]
18. Luchechko, A.; Zhydachevskyy, Y.; Sugak, D.; Kravets, O.; Martynyuk, N.; Popov, A.I.; Ubizskii, S.; Suchocki, A. Luminescence Properties and Decay Kinetics of $Mn^{2+}$ and $Eu^{3+}$ Co-Dopant Ions in $MgGa_2O_4$ Ceramics. *Latv. J. Phys. Tech. Sci.* **2019**, *55*, 43–51. [CrossRef]
19. Tawalare, P.K. Luminescent inorganic mixed borate phosphors materials for lighting. *Luminescence* **2022**, *37*, 1226–1245. [CrossRef]
20. Doke, G.; Krieke, G.; Antuzevics, A.; Sarakovskis, A.; Berzina, B. Optical properties of red-emitting long afterglow phosphor $Mg_2Si_{1-x}Ge_xO_4$: $Mn^{2+}/Mn^{4+}$. *Opt. Mater.* **2023**, *137*, 113500. [CrossRef]
21. Blasse, G.; Grabmaier, B.C. Luminescent Materials. In *Handbook of Electronic and Photonic Materials*; Springer: Berlin/Heidelberg, Germany, 1994. [CrossRef]
22. Matsuzawa, T.; Aoki, Y.; Takeuchi, N.; Murayama, Y. A new long phosphorescent phosphor with high brightness, $SrAl_2O_4$: $Eu^{2+}$, $Dy^{3+}$. *J. Electrochem. Soc.* **1996**, *143*, 2670. [CrossRef]
23. Andre, J.; Owens, D.A. The twilight envelope: A user-centered approach to describing roadway illumination at night. *Hum. Factors* **2001**, *43*, 620–630. [CrossRef]
24. Bachanek, K.H.; Tundys, B.; Wiśniewski, T.; Puzio, E.; Marouškova, A. Intelligent street lighting in a smart city concepts—A direction to energy saving in cities: An overview and case study. *Energies* **2021**, *14*, 3018. [CrossRef]
25. Looney, B. *Full Report—BP Statistical Review of World Energy 2020*; BP: London, UK, 2020; Available online: https://www.google.es/url?sa=t&rct=j&q=&esrc=s&source=web&cd=&cad=rja&uact=8&ved=2ahUKEwiagPDxka2BAxV3U6QEHRurA-AQFnoECA4QAQ&url=https%3A%2F%2Fwww.bp.com%2Fen%2Fglobal%2Fcorporate%2Fenergy-economics%2Fstatistical-review-of-world-energy.html&usg=AOvVaw3atGEVn2fNsaovzQJcj_OX&opi=89978449 (accessed on 11 August 2023).
26. Zissis, G. Energy Consumption and Environmental and Economic Impact of Lighting: The Current Situation. In *Handbook of Advanced Lighting Technology*; Springer: Cham, Switzerland, 2016; pp. 1–13.
27. Sadeghian, O.; Moradzadeh, A.; Mohammadi-Ivatloo, B.; Abapour, M.; Anvari-Moghaddam, A.; Shiun Lim, J.; Garcia Marquez, F.P. A comprehensive review on energy saving options and saving potential in low voltage electricity distribution networks: Building and public lighting. *Sustain. Cities Soc.* **2021**, *72*, 103064. [CrossRef]
28. Belloni, E.; Cotana, F.; Nakamura, S.; Pisello, A.L.; Villacci, D. A new smart laser photoluminescent light (LPL) technology for the optimization of the on-street lighting performance and the maximum energy saving: Development of a prototype and field tests. *Sustain. Energy Grids Netw.* **2023**, *34*, 101064. [CrossRef]
29. Ardavani, O.; Zerefos, S.; Doulos, L.T. Redesigning the exterior lighting as part of the urban landscape: The role of transgenic bioluminescent plants in mediterranean urban and suburban lighting environments. *J. Clean. Prod.* **2020**, *242*, 118477. [CrossRef]

30. Yeung, P. The French Town Where the Lighting Is Alive, 11th April 2022. Available online: https://www.bbc.com/future/article/20220407-the-living-lights-that-could-reduce-energy-use (accessed on 14 August 2023).
31. Praticò, F.G.; Vaiana, R.; Noto, S. Photoluminescent Road Coatings for Open-Graded and Dense-Graded Asphalts: Theoretical and Experimental Investigation. *J. Mater. Civ. Eng.* **2018**, *30*, 04018173. [CrossRef]
32. Gutiérrez, E.; Colorado, H. Development and Characterization of a Luminescent Coating for Asphalt Pavements. In *Characterization of Minerals, Metals, and Materials*; Springer: Cham, Switzerland, 2020; pp. 511–519. [CrossRef]
33. Giuliani, F.; Autelitano, F. Revêtements routiers photoluminescents: Étude expérimentale préliminaire en laboratoire. *Matériaux Tech.* **2014**, *102*, 603. [CrossRef]
34. Chiatti, C.; Fabiani, C.; Cotana, F.; Pisello, A.L. Exploring the potential of photoluminescence for urban passive cooling and lighting applications: A new approach towards materials' optimization. *Energy* **2021**, *231*, 120815. [CrossRef]
35. Sanjuán, M.A.; Argiz, C. Cementos fotoluminiscentes. *Afinidad* **2019**, *76*, 588.
36. Rosas-Casarez, C.A.; Arredondo-Rea, S.P.; Ramos-Ortiz, G.; Corral-Higuera, R.; Cruz-Enríquez, A.; Gómez-Soberón, J.M.; Velusamy, J.; Zárraga-Núñez, R.A.; Campos-Gaxiola, J.J. Excitation-dependent photoluminescent properties in geopolymers with addition of $Eu^{2+}$ $Dy^{3+}$ co-doped strontium silicoaluminate. *Mater. Lett.* **2019**, *250*, 170–173. [CrossRef]
37. *UNE 23035-1:2003*; Equipment for Fire Protection. Longtime afterglowing Signs. Part 1: Measurement and Marking. AENOR Standard: Madrid, Spain, 2003.
38. Gao, Y.; He, B.; Xiao, M.; Fang, Z.; Dai, K. Study on properties and mechanisms of luminescent cement-based pavement materials with super-hydrophobic function. *Constr. Build. Mater.* **2018**, *165*, 548–559. [CrossRef]
39. *UNE-EN 13036-1*; Road and Airfield Surface Characteristics—Test Methods—Part 1: Measurement of Pavement Surface Macrotexture Depth using a Volumetric Patch Technique. AENOR Standard: Madrid, Spain, 2010.
40. Praticò, F.G.; Astolfi, A. A new and simplified approach to assess the pavement surface micro-and macrotexture. *Constr. Build. Mater.* **2017**, *148*, 476–483. [CrossRef]


**Disclaimer/Publisher's Note:** The statements, opinions and data contained in all publications are solely those of the individual author(s) and contributor(s) and not of MDPI and/or the editor(s). MDPI and/or the editor(s) disclaim responsibility for any injury to people or property resulting from any ideas, methods, instructions or products referred to in the content.